

Physics
Electricity & Magnetism fields

Okayama University

Year 2003

The shielding effect of HTS power cable
based on E-J power law

Daisuke Miyagi* Satoru Iwata† Tomohiro Wakatsuki‡
Norio Takahashi** Shinji Torii††
Kiyotaka Ueda‡‡ Kenji Yasuda§

*Okayama University

†Okayama University

‡Okayama University

**Okayama University

††Central Research Institute of Electric Power Industry

‡‡Central Research Institute of Electric Power Industry

§Engineering Research Association for Superconductive Generation Equipment and Materials

This paper is posted at eScholarship@OUDIR : Okayama University Digital Information Repository.

http://escholarship.lib.okayama-u.ac.jp/electricity_and_magnetism/36

The Shielding Effect of HTS Power Cable Based on E - J Power Law

Daisuke Miyagi, Satoru Iwata, Tomohiro Wakatsuki, Norio Takahashi, *Fellow, IEEE*, Shinji Torii, Kiyotaka Ueda, and Kenji Yasuda

Abstract—A method for analysing the current distribution in high- T_c superconducting (HTS) power cable is examined by the aid of the novel use of anisotropic conductivity and 3-D finite element method considering E - J power law characteristic. The detailed current distribution in the cable is illustrated and the shielding effect of HTS shield layer with intervals is also examined. It is shown that AC losses in shield layer with intervals are increased when the interval between wires becomes large.

Index Terms— E - J power law characteristic, HTS power cable, HTS shield, 3-D finite element analysis.

I. INTRODUCTION

A SUPERCONDUCTING power cable is one of the most promising applications of high- T_c superconductor (HTS). However, the basic structure of an HTS cable is not established yet. To understand the electromagnetic characteristic of the HTS power cable correctly is important in order to realize a low cost and high efficiency HTS power cable [1]. The HTS power cable has magnetic shield layers composed of HTS wires in the exterior of conductor layers. This magnetic shield layer plays to prevent the increase of AC loss due to apply the magnetic field to the other phase conductor cores, and also to prevent the eddy current loss induced in heat insulation metal pipes. The number of superconducting wires n_s in the shield layer in the conventional HTS cable is larger than n_c in the conductor layer, because the radius of the shield layer is large compared with that of conductor layer. By the way, the shielding effect can be acquired by using the same number of superconductive wires of the shield layer as that of the conductor layer. If the shield layer with intervals having same number of superconducting wires with that of conductor layer is used, the cable cost can be cut down considerably. To design an efficient cable, the shielding effect should be exactly investigated by analysing, for example, the effect of twist pitch and the number of wires of a shield layer etc. on flux and current distributions. However, the report about the ac-

Manuscript received October 21, 2003. This work has been carried out as a part of Super-ACE (R&D of fundamental technologies for superconducting AC power equipment) project of METI, being consigned by NEDO.

D. Miyagi, S. Iwata, T. Wakatsuki, and N. Takahashi are with the Department of Electrical and Electronic Engineering, Okayama University, Okayama 700-8530, Japan (e-mail: miyagi@eplab.elec.okayama-u.ac.jp; iwata@eplab.elec.okayama-u.ac.jp; wakatsuki@eplab.elec.okayama-u.ac.jp; norio@eplab.elec.okayama-u.ac.jp).

S. Torii and K. Ueda are with the Komae Research Laboratory, Central Research Institute of Electric Power Industry, Tokyo 201-8511, Japan (e-mail: tori@criepi.denken.or.jp; uyeda@criepi.denken.or.jp).

K. Yasuda is with the Super-GM (Engineering Research Association for Superconductive Generation Equipment and Materials), Osaka 530-0047, Japan (e-mail: LDM04314@nifty.ne.jp).

Digital Object Identifier 10.1109/TASC.2004.830019

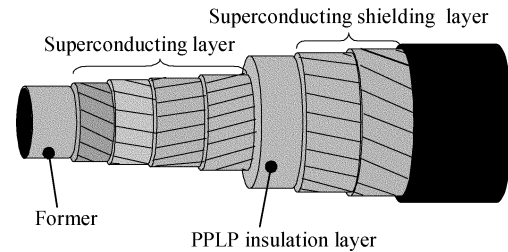


Fig. 1. Structure of typical HTS cable composed of multi-layered conductors.

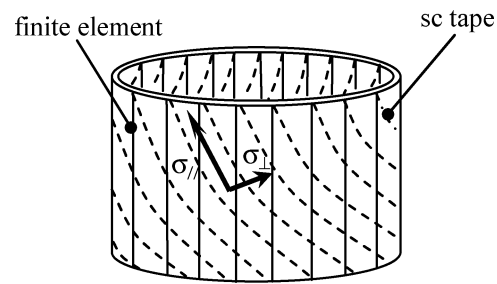


Fig. 2. Modeling of cable conductors with anisotropy of conductivity.

curate analysis of current distribution of the HTS cable taking account of the E - J characteristic is few reported [2], [3]. This is mainly because the 3-D analysis of current distribution in the HTS cable consisting of super-conducting tapes spirally wound on a former is not easy.

In this paper, 3-D finite element analysis taking account of the nonlinear E - J power law characteristic is carried out by modeling the spirally wound superconducting tapes as the conductors having an anisotropic conductivity [4], [5]. The detailed current distribution in the cable is illustrated. The effect of number of superconducting wires in the HTS shield layer with intervals on the shielding characteristics is discussed.

II. METHOD OF ANALYSIS

A. Modeling of Cable Structure

An HTS cable should consist of multi-layered conductors to increase its current loading. The structure of typical HTS cable is shown in Fig. 1. When there are many layers of superconductor in a superconducting cable, it is difficult to analyze magnetic fields in the cable using the conventional 3-D finite element method, because the number of finite elements increases greatly. If the cable is treated as a macroscopic one having anisotropic conductivity as shown in Fig. 2, the calculation can be carried out within the acceptable memory requirement and CPU time. Moreover, since it is not necessary to gen-

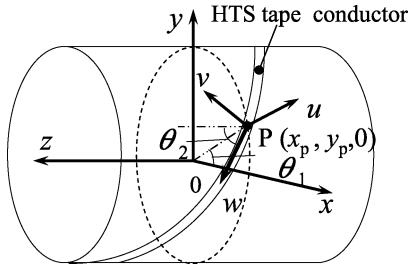


Fig. 3. Local coordinates.

erate a mesh even if the twist pitch is changed, the optimal twist pitch can be easily examined.

The conductivity $\sigma_{//}$ parallel to the superconducting tape depends on the *E-J* power law characteristic. The conductivity σ_{\perp} perpendicular to the superconducting tape is assumed by

$$\sigma_{\perp} = \frac{\sigma_{//}\sigma_m}{\lambda\sigma_m - (1 - \lambda)\sigma_{//}} \quad (1)$$

where σ_m is the conductivity of the silver sheath. λ is the volume fraction of superconductor in the HTS layer. The conductivity σ_m of silver sheath is 3.45×10^8 S/m (at 77 K) and the volume fraction λ is assumed as equal to 0.6.

The conductivity of the anisotropic conductor is a tensor, of which the off-diagonal elements are all zero. The current density J_u , J_v and J_w in the *u*-, *v*- and *w*-directions defined along the superconducting tape as shown in Fig. 3 can be written using each component E_u , E_v and E_w of electric field strength E and σ_{\perp} and $\sigma_{//}$ as follows [5]:

$$\begin{Bmatrix} J_u \\ J_v \\ J_w \end{Bmatrix} = \begin{bmatrix} \sigma_{\perp} & 0 & 0 \\ 0 & \sigma_{\perp} & 0 \\ 0 & 0 & \sigma_{//} \end{bmatrix} \begin{Bmatrix} E_u \\ E_v \\ E_w \end{Bmatrix}. \quad (2)$$

The relationship between J_x , J_y and J_z and E_x , E_y and E_z can be obtained as follows [5]:

$$\begin{aligned} \begin{Bmatrix} J_x \\ J_y \\ J_z \end{Bmatrix} &= [K] \begin{bmatrix} \sigma_{\perp} & 0 & 0 \\ 0 & \sigma_{\perp} & 0 \\ 0 & 0 & \sigma_{//} \end{bmatrix} [K]^{-1} \begin{Bmatrix} E_x \\ E_y \\ E_z \end{Bmatrix} \\ &= \begin{bmatrix} \sigma_a & \sigma_b & \sigma_c \\ \sigma_d & \sigma_e & \sigma_f \\ \sigma_g & \sigma_h & \sigma_i \end{bmatrix} \begin{Bmatrix} E_x \\ E_y \\ E_z \end{Bmatrix} \end{aligned} \quad (3)$$

where $[K]$ is the transformation matrix [5].

B. Model of HTS Power Cable

Fig. 4 shows the analyzed model. We assume three kinds of models of HTS power cables. All models have same dimensions of conductor layer. The difference between each model is the structure of the HTS shield layer. The model I has the conventional shield layer of which the HTS tapes are fully would. The models II and III have shield layers with intervals. Table I shows the specifications of each model. Table II shows the specifications of HTS tape wire which constitutes the conductor layer and shield layer. The width of HTS tape wire of both conductor and shield layers is 4 mm. The thickness of HTS tape wire of the conductor layer is 0.2 mm and that of the shield layer is 0.24 mm. The inner radii of the conductor layer and the shield layer are

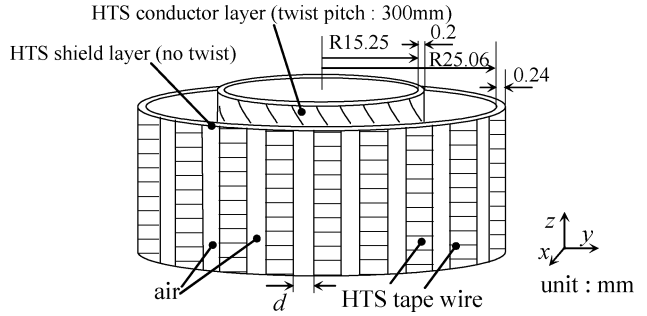


Fig. 4. Model of HTS power cable composed of 1-layer HTS conductor with twist and 1-layer HTS shield without twist.

TABLE I
SPECIFICATIONS AND CONDITIONS OF HTS
CABLE MODEL FOR NUMERICAL ANALYSIS

Model	I	II	III
Number of divisions in radial direction	125	125	125
Number of divisions in circumferential direction	4	64	76
Number of elements	426	6816	8094
Number of nodes	1072	13912	16480
Number of HTS tape wires in a shield layer	40	32	20
Interval between wires in a shield layer : d (mm)	0	0.94	4.0
Twist pitch of a shield layer	No	No	No
Number of HTS tape wires in a conductor layer	23	23	23
Twist pitch of a conductor layer L_p (mm)	300	300	300

TABLE II
SPECIFICATIONS OF HTS TAPE WIRE

Dimension (mm ²) in conductor layer	4.0 × 0.2
Dimension (mm ²) in shield layer	4.0 × 0.24
Critical current density J_c (A/m ²)	4.0×10^7
n value	8

15.25 mm and 25.06 mm, respectively. The critical current density J_c and n value of a conductor layer and a shield layer are both equal to 4.0×10^7 A/m² and 8, respectively.

The conductor layer consists of 23 HTS tape wires and twist pitch is 300 mm. It is assumed that the conductor layer is composed of HTS tapes which is fully covered on the former surface, without leaving a crevice. As shown in Fig. 4 and Table I, shield layers of all models are not twisted. The shield layer of model I is composed of 40 HTS tape wires without leaving a crevice. The shield layers of model II and III are composed of 32 and 20 HTS tape wires with equal intervals, respectively. The applied transport current is sinusoidal ($I_p \sin \omega t$) and the frequency is 50 Hz. The peak value of transport current I_p is equal to $0.8 I_c$ (I_c : critical current).

A small sector (1/180, 1/32, 1/20 regions for models I, II and III) is analyzed due to symmetry by utilizing the periodic boundary condition. The superconducting cable is treated as a conductor having large conductivity. The magnetic field is analyzed using the 3-D edge-based hexahedral finite element method (A- ϕ method, A: magnetic vector potential, ϕ : electric

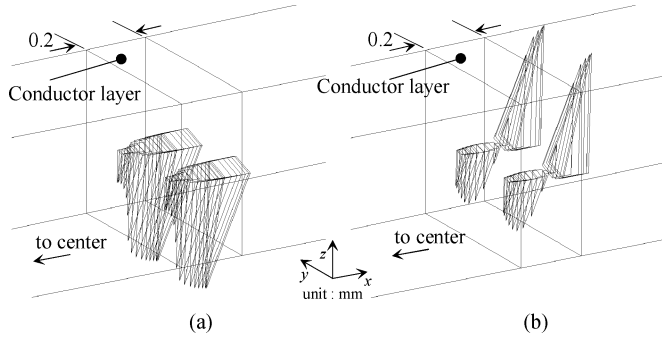


Fig. 5. AC current distributions in conductor layer at model I (n value = 8, $L_p = 300$). (a) $\omega t = -\pi/2$ ($|J_{\max}| = 4.37 \times 10^7$ A/m²). (b) $\omega t = 0$ ($|J_{\max}| = 4.14 \times 10^7$ A/m²).

scalar potential). The convergence criterion of ICCG method is chosen as 10^{-8} .

C. Conductivity of Superconductor to be Used in Numerical Analysis

The infinite conductivity $\sigma_{//}$ of the superconductor cannot be treated in the numerical calculation. Then, one needs to determine a suitable value for the conductivity $\sigma_{//}$ in (2) for the numerical analysis. The superconducting property is given by the E - J characteristic represented with a power law as follows:

$$E = E_c \left(\frac{J}{J_c} \right)^n \quad (4)$$

where E_c is assumed as equal to 1×10^{-4} V/m. Then, the equivalent conductivity of superconductor $\sigma_{//}$ is derived as,

$$\sigma_{//} = \frac{J}{E} = \frac{J_c^n}{E_c} J^{1-n}. \quad (5)$$

$\sigma_{//}$ is determined iteratively at each time step $\Delta t (= 5 \times 10^{-4}$ sec) until the final result is obtained. The conductivity $\sigma_{//}^{(k)}$ at the k -th iteration is given by

$$\sigma_{//}^{(k)} = \sigma_{//}^{(k-1)} + \alpha \left(\sigma_{//}^* - \sigma_{//}^{(k-1)} \right) \quad (6)$$

where $\sigma_{//}^*$ is the conductivity calculated using (5). α is the under relaxation factor ($\alpha = 0.1$). The iteration is stopped, when $\sigma_{//}^* - \sigma_{//}^{(k-1)}$ becomes less than 0.05. To enhance the efficiency of calculation, the maximum value of $\sigma_{//}$ is limited to 1.0×10^{12} S/m and the minimum value of $\sigma_{//}$ is limited to the conductivity σ_m of silver sheath. Within 100 iterations in average are necessary to obtain the current distribution considering the E - J characteristics.

III. NUMERICAL ANALYSIS AND DISCUSSION

A. Current Distribution in a Conductor Layer

Fig. 5 shows the current distribution in the conductor layer of model I at $\omega t = -\pi/2$ (transport current I is equal to minus peak value) and at $\omega t = 0$ (I is equal to zero). Fig. 5 denotes that the current diffuses into the conductor layer from the outer surface and it flows in the twist direction. The maximum value of current density $|J_{\max}|$ is slightly larger than $J_c (= 4.0 \times 10^7$ A/m²).

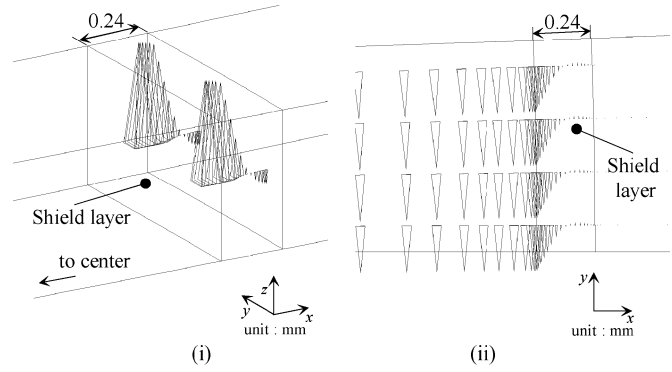


Fig. 6. Flux and current distributions in a shield layer of model I (model I: 40 HTS tape wire without interval between wires in a shield layer, $d = 0$ mm, at $\omega t = -\pi/2$, n value = 8). (i) Current distribution in a shield layer; (ii) flux distribution around a shield layer.

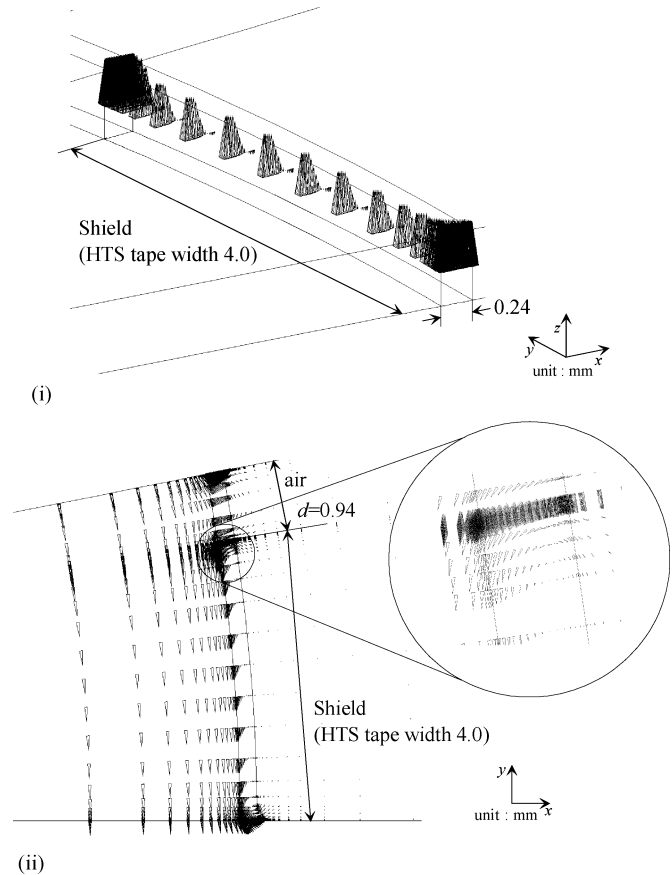


Fig. 7. Flux and current distributions in a shield layer of model II (model II: 32 HTS tape wires in a shield layer, $d = 0.94$ mm, at $\omega t = -\pi/2$, n value = 8). (i) Current distribution in a shield layer; (ii) flux distribution around a shield layer.

B. Shielding Effect of Shield Layer With Intervals

The current distributions in three kinds of HTS shield layers of HTS power cable model are analyzed. Figs. 6, 7 and 8 show the current and flux distributions of three models (composed of 40 HTS tape wires), model I having shield layer without intervals between wires, model II having shield layer composed of 32 HTS tape wires and model III having shield layer composed of 20 HTS tape wires. As shown in Fig. 6, the shield layer of model I has a very high shielding effect. If the interval between

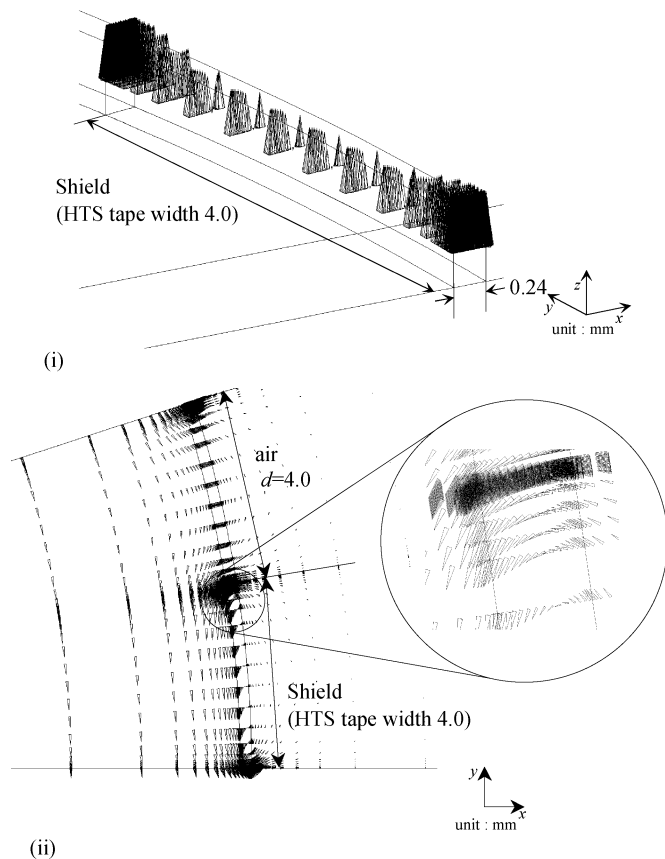


Fig. 8. Flux and current distributions in a shield layer of model III (model III : 20 HTS tape wires in a shield layer, $d = 4.0$ mm, at $\omega t = -\pi/2$, n value = 8). (i) Current distribution in a shield layer; (ii) flux distribution around a shield layer.

wires is increased, the shield effect decreases as shown in Fig. 8. Fig. 7 denotes that the shielding layer having 32 HTS wires ($d = 0.94$ mm) is sufficient for the shielding of leakage flux. Figs. 7 and 8 denote that the magnetic field perpendicular to the HTS tape surface increases at the edge of the wire superconductivity properties of HTS tape, and this cause the decrease of wire. The maximum flux density perpendicular to the surface of tape wire at peak transport current I_p is shown in Table III. The maximum flux density of model III is about twice as larger as that of model II.

As the flux penetrates into the shield layer as shown in Figs. 6, 7 and 8, the AC loss in the shield layer should be examined. The AC loss Q (W/m) is given by

$$Q = \int \frac{1}{T} \int_0^T \mathbf{E} \cdot \mathbf{J} dt dv, \quad (7)$$

TABLE III
FLUX DENSITY AND AC LOSS

Model	I	II	III
Maximum flux density perpendicular to the surface of HTS tape wire at transport current peak. (T)	-	4.0×10^{-3}	7.4×10^{-3}
AC loss of a shield layer at $I_p = 0.5I_c$ (W/m)	0.58×10^{-2}	0.66×10^{-2}	1.22×10^{-2}
AC loss of a shield layer at $I_p = 0.8I_c$ (W/m)	1.63×10^{-2}	1.98×10^{-2}	4.81×10^{-2}

where T is the period of one cycle. The AC loss of each model calculated by (7) at $I_p = 0.5I_c$ and $0.8I_c$ are shown in Table III. When the interval of between wires becomes large, the loss is increased. This suggests that the manufacturing cost is reduced but the running cost is increased due to the increase of AC loss, when the number of HTS tape wire in the shield layer is reduced.

IV. SUMMARY

A method for analysing the current distribution in high- T_c superconducting power cable is examined by the aid of novel use of anisotropic conductivity and 3-D finite element method in consideration of E - J power law characteristics. The detailed current and flux distribution in the cable are illustrated and the shielding effect of HTS shield is also examined. It is shown that the manufacturing cost is reduced but the running cost is increased due to the increase of AC loss, when the number of HTS tape wire in the shield layer is reduced. The results of our analysis will give an important information for the optimal design of HTS power cable.

REFERENCES

- [1] S. Honjo, K. Matsuo, T. Miura, and Y. Takahashi, "High- T_c superconducting power cable development," *Physica C*, no. 357–360, pp. 1234–1240, 2001.
- [2] S. Honjo, N. Hobara, Y. Takahashi, H. Hashimoto, K. Narita, and T. Yamada, "Efficient finite element analysis of electromagnetic properties in multi-layer superconducting power cables," *IEEE Trans. Appl. Supercond.*, vol. 13, no. 2, pp. 1894–1897, June 2003.
- [3] N. Amemiya, K. Miyamoto, S. Murasawa, H. Mukai, and K. Ohmatsu, "Finite element analysis of AC loss in nontwisted Bi-2223 tape carrying AC transport current and/or exposed to DC or AC external magnetic field," *Physica C*, vol. 310, pp. 30–35, 1998.
- [4] W. J. Carr Jr., *AC Loss and Macroscopic Theory of Superconductors*: Gordon and Breach Science Publishers, 1983.
- [5] N. Takahashi, T. Nakata, Y. Fujii, K. Muramatsu, M. Kitagawa, and J. Takehara, "3-D finite element analysis of coupling current in multifilamentary AC superconducting cable," *IEEE Trans. Magn.*, vol. 27, no. 5, pp. 4061–4064, 1991.